نشریه مهندسی مکانیک امیرکبیر

Amirkabir Journal of Mechanical Engineering

Amirkabir J. Mech. Eng., 54(10) (2023) 491-494
DOI: 10.22060/mej.2022.20581.7261

Presenting the Traction-Separation Law for Ultrasonic Welding of Glass-Fiber Reinforced Polypropylene Composite

R. Ahmadi, H. Biglari*

Department of Mechanical Engineering, University of Tabriz, Tabriz, Iran

ABSTRACT: The generalized progressive damage model is numerically and experimentally studied to predict the degradation process in end notch flexure composite specimens welded by the ultrasonic method. In numerical modeling, a trapezoidal traction-separation model that expresses the embedded process zone is developed using three data reduction methods of the compliance calibration method, classical beam theory, and compliance-based beam method, and formulated by combining failure and damage mechanics. Finally, the force-displacement diagrams obtained from experimental investigations and the force-displacement diagrams extracted from numerical modeling are compared. The results demonstrate that the models extracted using the compliance-based beam method and classical beam theory method make accurate predictions compared to the compliance calibration method.

Review History:
Received: Sep. 21, 2021
Revised: Sep. 02, 2022
Accepted: Sep. 10, 2022
Available Online: Oct. 04, 2022

Keywords:
Traction-separation
Mode II fracture
Ultrasonic welding

1- Introduction

In general, the bonding methods of thermoplastic composites can be divided into mechanical, adhesive joints, and welding.

The welding method has a high potential for bonding, assembly, and repairing thermoplastic composites and confers numerous advantages over other bonding methods. In addition, this method can significantly solve the problems caused by mechanical and adhesive methods.

A notable feature of the ultrasonic method is that the temperature remains lower than the melting temperature of the materials. Accordingly, the ultrasonic welding process is adopted to connect reinforced polypropylene composites with glass fibers in this research.

Since, in practice, discontinuities and cracks may occur in the weld layer, the traction-separation fracture law of the mode II weld layer is discussed using the adhesive theory.

In this study, the progressive damage model was numerically and experimentally investigated to predict the degradation process in an ultrasonically welded composite with End Notch Flexure (ENF) specimens. After performing the three-point bending test, energy values for crack growth and development were calculated using three data reduction methods Compliance Calibration Method (CCM), Classical Beam Theory (CBT), and Compliance-Based Beam Method (CBBM). Subsequently, the trapezoidal traction-separation model expressing the Embedded Process Area (EPZ) was calculated for each of these methods and modeled by Abacus finite-element software.

Table 1. Mechanical properties of glass-fiber-reinforced polypropylene composite

E_1 (MPa)	E_2 (MPa)	E_3 (MPa)
5150	2100	2100
ν_{12}	ν_{13}	ν_{23}
0.32	0.32	0.14
G_{12} (MPa)	G_{13} (MPa)	G_{23} (MPa)
400	400	1380

2- Experimental Setup

2- 1- Sample materials

The samples were made of polypropylene composite reinforced with glass fibers. The mechanical properties of the composite are presented in Table 1.

2- 2- Sample manufacturing

Composite sheets were made by the hot vacuum bag method. To produce the arms with dimensions of 140*20*2 mm, the composite sheets were cut with a pressure of 2000 psi using a 5-axis water jet cutting machine (Flow Company). ENF samples were produced by ultrasonic welding to connect the two arms.

Effective parameters in the ultrasonic welding of plastics include maintenance pressure, welding time, and amplitude of ultrasonic waves at three levels. To reduce the number

*Corresponding author's email: hbiglari@tabrizu.ac.ir

Table 2. Design of Experiments (DOE)

No. of Exp.	ENF Samples	*P* (bar)	*A* (μm)	*T* (s)
1	ENF 1	1.5	27	0.4
2	ENF 2	1.5	30	0.8
3	ENF 3	1.5	33	1.2
4	ENF 4	2	27	0.8
5	ENF 5	2	30	1.2
6	ENF 6	2	33	0.4
7	ENF 7	2.5	27	1.2
8	ENF 8	2.5	30	0.4
9	ENF 9	2.5	33	0.8

Fig. 1. Ultrasonic welding of the arms to make an ENF sample

of experiments while maintaining the quality of results, the above parameters were evaluated using the design of experiment methods (Table 2).

The device employed here was an ultrasonic welding press for welding plastics with a power of 2600 Watts and an ultrasonic wave frequency of 15 kHz. To create the initial crack, a 20μm non-stick sheet was employed during welding. The specimens were then placed inside the fixture and were welded with a rectangular horn in the dimensions of 30*100 mm. The experiments were repeated three times (Fig. 1) to ensure the accuracy of the experimental data.

2- 3- Three-point bending test (ENF)

2- 4- The ENF tests were performed by the AI-7000M tensile tester of GOTECH Taiwan Company with a displacement accuracy of 0.00004 mm and using a 20kN dynamometer. A controlled load was applied to the middle and downward at the constant rate of 0.1 mm/min.

3- Data Reduction Methods – Calculating the Energy Release Rate

The data reduction method was employed to calculate the energy release rate and the corresponding *R* curve. Three data reduction methods of CCM, CBT, and CBBM were adopted to calculate the energy release rate and the corresponding *R* curve in mode II.

The CCM, CBT, and CBBM methods use Eqs. (1) to (3) to calculate G_{II}, respectively.

$$G_{II} = \frac{3m\alpha^2 P^2}{2b} \tag{1}$$

$$G_{II} = \frac{9(\alpha + 0.42\Delta_1)^2 P^2}{16b^2 h^3 E_1} \tag{2}$$

$$G_{II} = \frac{9\alpha_e^2 P^2}{16b^2 h^3 E_f} \tag{3}$$

4- Results and Discussion

4- 1- Extracting traction-separation laws

. Fiber bridging can be expressed as the tension-separation or bridging law, which is a property of the material, derived from the *R* curve.

After calculating G_{II}, to describe the effect of the *R* curve by calculating the J integral around the crack tip and along with the crack plates while considering the presence of the bridging area, Suo et al. [1] obtained the following equations (Eqs. (4) to (6)) for the energy release rate in mode II:

$$G_{SS,II} = G_{0,II} + G_{b,II} \tag{4}$$

$$G_{b,II} = \int_0^{\delta_{II}^*} \sigma\left(\delta_{II}^*\right) d\delta_{II}^* \tag{5}$$

$$\sigma_{II}\left(\delta_{II}^*\right) = \frac{\partial G_{II}}{\partial \delta_{II}^*} \tag{6}$$

4- 2- Processing the experimental results

The experimental results obtained from the ENF tests were processed to calculate the critical failure energy and initial failure toughness. The $G_{II} - \delta_{II}^*$ diagram using the three data reduction methods CCM, CBT, and CBBM were calculated for different ENF samples.

for each ENF sample, an analytic function (fit function) that can estimate the procedure of changes was presented according to the format of Eq. (7) [2]. This procedure is required for using Eq. (6) and, therefore, creates an analytical form of bridging laws.

$$G_{II} - \delta_{II}^* \tag{7}$$

Using the diagram G_{II}-δ^*_{II} and Eq. (6), the bridging law σ_{II}-δ^*_{II} for all the samples can be obtained. Differentiation from the second-order polynomial function with respect to δ^*_{II} creates linear bridging laws. Fig. 2 compares the bridging

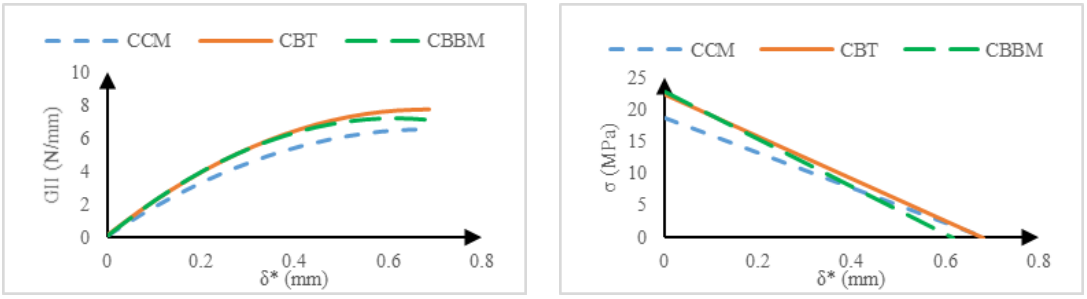

Fig. 2. Fit diagram of GII-δ*II and experimental bridging laws calculated for ENF 3 sample using three data reduction methods

Table 3. Experimental parameters obtained from bridging mode II laws for ENF 3 sample

	ENF 3	
	$\sigma_{C,II}$ (MPa)	$\delta^*_{C,II}$ (mm)
CCM	18.732	0.687514
CBT	22.305	0.682569
CBBM	22.935	0.61587

laws derived from the CCM, CBT, and CBBM data reduction methods for ENF 3 sample.

Table 3 presents the bridging stress at the onset of crack growth and the critical slip displacement obtained from the bridging mode II laws for the ENF 3 sample.

4- 3- Bridging and cohesive zones' model

A cohesive zone model with a trapezoidal traction-separation response is accepted in this work over the usual adopted bilinear CZM to define the deformation and damage growth .(process in the thermoplastic ultrasonic welding layer (Fig. 3

The traction-separation law in ABAQUS is defined by the damage variable (D) according to Eq. (8),

$$\sigma = (1-D)K\delta \tag{8}$$

Therefore, the damage variable is expressed for the traction-separation diagram defined according to Eq. (9) [3]:

$$D=\begin{cases} 0 & for \quad 0<\delta<\delta_{0,II} \\ 1-\dfrac{\delta_{0,II}}{\delta} & for \quad \delta_{0,II}<\delta<\delta_{1,II} \\ 1-\dfrac{\delta_{0,II}}{\delta}\dfrac{\delta_{C,II}-\delta}{\delta_{C,II}-\delta_{1,II}} & for \quad \delta_{1,II}<\delta<\delta_{C,II} \\ 1 & for \quad \delta>\delta_{C,II} \end{cases} \tag{9}$$

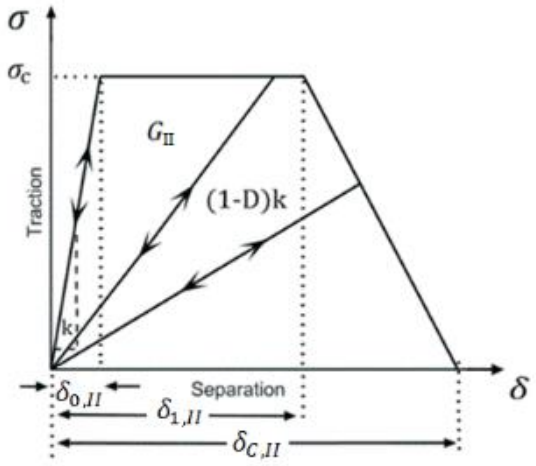

Fig. 3. Trapezoidal traction-separation law

References

[1] Z. Suo, G. Bao, B. Fan, Delamination R-Curve Phenomena Due to Damage, Journal of the Mechanics and Physics of Solids, 40(1) (1992) 1-16.

[2] K.N. Anyfantis, N.G. Tsouvalis, Experimental and numerical investigation of Mode II fracture in fibrous reinforced composites, Journal of reinforced plastics and composites, 30(6) (2011) 473-487.

[3] M. De Moura, J. Gonçalves, J. Chousal, R. Campilho, Cohesive and continuum mixed-mode damage models applied to the simulation of the mechanical behaviour of bonded joints, International Journal of adhesion and Adhesives, 28(8) (2008) 419-426.

HOW TO CITE THIS ARTICLE
R. Ahmadi, H. Biglari, Presenting the Traction-Separation Law for Ultrasonic Welding of Glass-Fiber Reinforced Polypropylene Composite, Amirkabir J. Mech Eng., 54(10) (2023) 491-494.

DOI: 10.22060/mej.2022.20581.7261